DETC2019-97601

ACTUATED DUAL-SLIP MODEL OF PLANAR SLOPE WALKING

Raul Lema Galindo

Mechanical Engineering University of Texas at Austin Austin, TX 78712-1591 Email: rlema@utexas.edu

Elise Weimholt

Aerospace & Mechanical Engineering Aerospace & Mechanical Engineering University of Notre Dame Notre Dame, IN 46556 Email: eweimhol@nd.edu

James P. Schmiedeler*

University of Notre Dame Notre Dame, IN 46556 Email: schmiedeler.4@nd.edu

ABSTRACT

The planar dual spring-loaded inverted pendulum (dual-SLIP) model is a well-established passive template of human walking on flat ground. This paper applies an actuated extension of the model to walking on inclines and declines to evaluate how well it captures the behavior observed in human slope walking. The motivation is to apply the template to improve control of humanoid robot walking and/or intent detection in exoskeletonassisted walking. Gaits of the actuated planar dual-SLIP model are found via the solution of a constrained nonlinear optimization problem in ten parameters. The majority of those parameters define the actuation scheme that injects energy for incline walking and absorbs energy for decline walking to achieve periodic, nonconservative gaits. Solution gaits across the speed range of 1.0 to 1.6 $\frac{m}{s}$ and slope range of -10 to 10 degrees exhibit some of the characteristics of human walking, such as the effect of slope on stance duration, step frequency, and step length. Efforts to reduce the number of parameters optimized by enforcing relationships observed in the solution gaits proved unsuccessful, suggesting that future work must trade off model complexity with fidelity of representation of human behavior.

INTRODUCTION

Human walking is well known to involve the cyclic exchange of gravitational potential energy and the kinetic energy of forward motion. The dual spring-loaded inverted pendulum (dual-SLIP) model consists of a single point mass, representing the mass of the entire body, to which two massless linear springs, representing the legs, are attached [1]. This model better captures the sagittal plane characteristics of walking than does the simpler rigid inverted pendulum model of walking. These characteristics include the vertical displacement of the center of mass, the twopeaked nature of the vertical ground reaction forces, and the nonzero duration of the double support phase. The dual-SLIP model is passive, so no control action is required to find steady-state periodic solutions for walking with the model across a range of speeds over level ground. It also offers the benefit of being consistent with the dynamics of running, such that a single model is representative of walking (alternating single and double support phases) and running (alternating single support and flight phases).

While the dual-SLIP model was originally conceived to be planar, it has also been extended to three dimensions by specifying two angles for leg touchdown instead of just one [2]. This extension did result in the loss of the self-stable behavior of the planar gaits, but an LQR controller was found to stabilize the spatial dynamics and enhance robustness to disturbances. A number of actuation approaches have also been introduced so that the dual-SLIP model can be extended to represent non-conservative walking, such as on uneven or inclined/declined terrain. These approaches range from discrete changes to the rest length of the leg spring during double support [2] to linear changes in the rest length across one or more phases of stance [3]. A common feature of the approaches is that they allow the leg springs in the model to touch down and lift off at lengths other than their free lengths. The motivation for the extension to an actuated

^{*}Address all correspondence to this author.

model was originally to improve the gait generation and control of humanoid robots, particularly for walking over uneven terrain either without terrain sensing or with uncertainty in that sensing [4]. The authors' ongoing work, however, is examining how this more flexible model can likewise improve intent detection in robot-assisted locomotion, be that with exoskeletons or powered lower-limb prostheses [5].

Decline walking is of particular interest in rehabilitation applications [6], in part because the decrease in gravitational potential energy with every step requires the lower-limb muscles to absorb energy if the forward velocity is to remain constant [7]. Muscles absorb energy by performing negative work via eccentric contractions. These are characterized by muscle activation at a level that produces a muscle force less than the externally induced load such that the active muscle lengthens rather than contracting. Eccentric activity is particularly prevalent in the weight acceptance phase of gait, which is roughly the first 20-30% of stance [8]. Therefore, it is unsurprising that healthy humans modify their postural and joint kinematics in the weight acceptance phase when walking on declines. Specifically, they exhibit a reduction in hip flexion at foot touchdown and an increase in knee flexion during weight acceptance, which both contribute to a decrease in stride length [9]. Individuals with spinal cord injury typically do not adopt these same adaptations [10], though, perhaps because of the added challenges of performing eccentric contractions with the sensory and neural deficits that often accompany spinal cord injury.

This work aims to determine if the actuated planar dual-SLIP model can capture the key characteristics of healthy human gait on incline and decline surfaces. Demonstration of those characteristics within the model would help validate its utility as a template for control of biped robot walking on slopes. It would also support use of the model as a template within intent detection algorithms for exoskeletons and powered lower-limb prostheses. The remainder of the paper is organized as follows. The following section introduces the mathematics of the actuated planar dual-SLIP model. Then, the approach to finding periodic gaits via numerical optimization is described. In the next section, results for a variety of slopes are provided, and the paper ends with conclusions and discussion of future work.

ACTUATED DUAL-SLIP MODEL

As shown in Fig. 1, the dual-SLIP model is composed of a point mass m and two massless spring legs, each with linear stiffness k. For consistency of the analysis herein with the level ground results from Geyer, et al. [1], body mass is assumed to be m=80 kg, and spring stiffness is assumed to be k=20 kN/m. Free leg length is nominally 1 m, but since it is allowed to vary, that is truly just a nominal value. The coordinate system is established with the x-axis parallel to the ground in the direction of forward progression and the y-axis perpendicular to the ground. The x

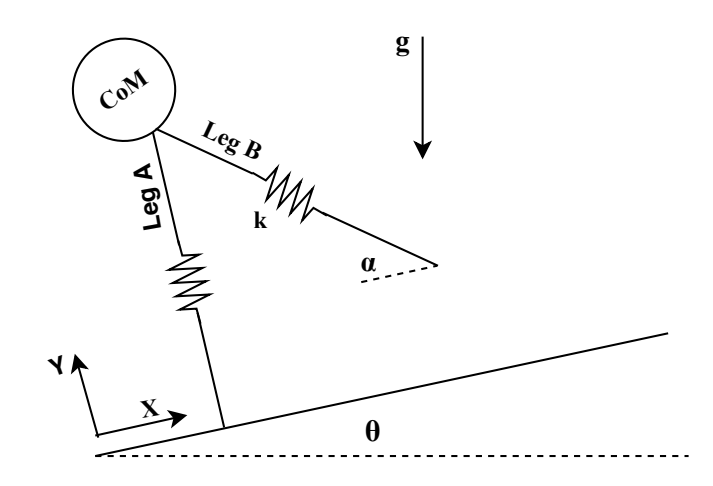


FIGURE 1: Dual-SLIP model of walking on incline terrain.

and y coordinates identify the position of the point mass relative to an inertial reference frame, and derivatives with respect to time are indicated with the dot notation. The slope of the terrain is denoted by the angle θ measured positive counter-clockwise from the horizontal, so θ is negative for decline walking. The acceleration of gravity is g. The angle of the swing leg at touchdown is α , which is measured positive clockwise from the ground for consistency with [1].

Assuming left-right symmetry for steady-state, periodic walking, only one complete step of the stride cycle need be analyzed. It is convenient to begin the analysis at mid-stance (MS) of the trailing leg, which is the leg that trails in position relative to the other during their eventual double support phase. (It leads in time in terms of its touchdown relative to the other leg.) In Fig. 1, Leg A is the trailing leg. Mid-stance is defined as occurring when the component of the center-of-mass velocity perpendicular to the ground vanishes, $\dot{y} = 0$. On level ground, symmetry dictates that this occurs when the stance leg is vertical, which significantly simplifies the analysis. In slope walking, however, \dot{y} is not necessarily zero when the stance leg is vertical or perpendicular to the ground. One complete step begins at mid-stance of Leg A and ends at mid-stance of Leg B, with phases of single support for Leg A (SS_A) , double support (DS), and single support for Leg B (SS_B) as shown in Fig. 2.

Single Support of Leg A

If the origin of the inertial reference frame is placed at the point of contact between trailing Leg A and the ground (Leg A's touchdown position), the equations of motion in the single support phase of Leg A are

$$\ddot{x} = \frac{Px}{m} - g\sin\theta,\tag{1}$$

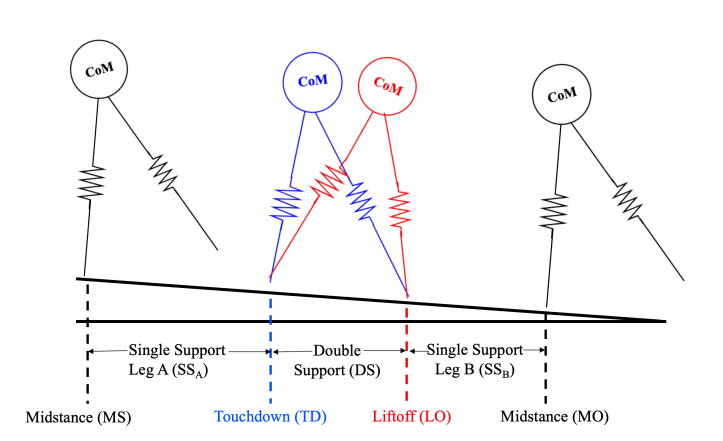


FIGURE 2: Phases of gait analyzed with the actuated dual-SLIP model shown walking down a decline.

$$\ddot{y} = \frac{Py}{m} - g\cos\theta,\tag{2}$$

where

$$P = k \left(\frac{\ell_A}{\sqrt{x^2 + y^2}} - 1 \right) \tag{3}$$

following the notation of [1] to express the leg spring force more compactly in Eq. 2 and ℓ_A is the time-varying free length of Leg A. In the actuated model, ℓ_A varies linearly from mid-stance to lift-off,

$$\ell_A = \ell_{MS} + \beta_A t, \tag{4}$$

where ℓ_{MS} is the free length of Leg A at mid-stance and β_A is the rate of change of ℓ_A as a function of time t. Figure 3 graphically depicts the changes in free length and actual leg length across the different phases of gait.

Double Support

The touchdown of Leg B occurs when

$$y = L_{TD} \sin \alpha, \tag{5}$$

where L_{TD} is the actual length of the leg at touchdown, which is not in general the same as the free length of the leg at touchdown,

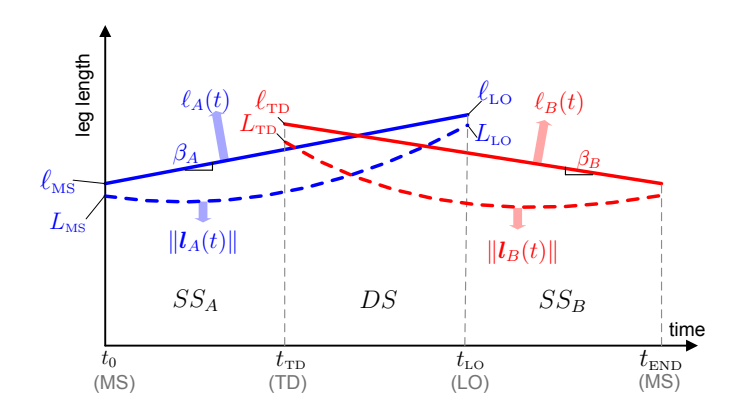


FIGURE 3: Illustration of the quantities governing the actuation of the leg springs. The trailing Leg A quantities are shown in blue, while the leading Leg B quantities are shown in red. Solid lines indicate free lengths of the springs, and dashed lines indicate actual leg lengths.

 ℓ_{TD} , for the actuated model. Differences in ℓ_{TD} and L_{TD} lead to discontinuities in the ground reaction forces that mimic the impact forces that would be seen in a model with a massive foot and/or leg. The equations of motion in double support are

$$\ddot{x} = \frac{Px - Q(d - x)}{m} - g\sin\theta,\tag{6}$$

$$\ddot{y} = \frac{Py + Qy}{m} - g\cos\theta,\tag{7}$$

where

$$Q = k \left(\frac{\ell_B}{\sqrt{(d-x)^2 + y^2}} - 1 \right), \tag{8}$$

again following the notation of [1] for compactness of the spring force terms, ℓ_B is the time-varying free length of Leg B,

$$\ell_B = \ell_{TD} + \beta_B (t - t_{TD}), \tag{9}$$

 β_B is the rate of change of ℓ_B as a function of time, t_{TD} is the time at which touchdown of Leg B occurs, d is the position of the point of contact of Leg B relative to the origin (d is equal to the step length),

$$d = x_{TD} + L_{TD}\cos\alpha,\tag{10}$$

and x_{TD} is the position of the point mass at touchdown of Leg B.

Single Support of Leg B

The lift-off of Leg A occurs when its length is equal to the lift-off leg length L_{LO} ,

$$L_{LO} = \sqrt{x^2 + y^2},$$
 (11)

which in general is not equal to the free length ℓ_{LO} at the time of lift-off. Differences in ℓ_{LO} and L_{LO} lead to discontinuities in the ground reaction forces that are similar to the small rise in force due to late stance push-off in humans, which isn't captured in the passive dual-SLIP model. Following the lift-off of Leg A, the equations of motion for the single support phase of Leg B are

$$\ddot{x} = -\frac{Q(d-x)}{m} - g\sin\theta,\tag{12}$$

$$\ddot{y} = \frac{Qy}{m} - g\cos\theta. \tag{13}$$

Mid-stance of Leg B occurs when $\dot{y} = 0$, which is the end of the single step analyzed.

PERIODIC WALKING GAITS

The equations of motion in Eqs. 1 and 2 can be integrated forward from time t = 0 until Eq. 5 is satisfied, triggering the start of double support. Likewise, Eqs. 6 and 7 can then be integrated forward in time until Eq. 11 is satisfied, triggering the start of single support of Leg B. Lastly, Eqs. 12 and 13 can be integrated forward in time until $\dot{y} = 0$, indicating the next mid-stance. Finding periodic walking gaits amounts to solving a nonlinear optimization problem to find the parameters listed in Table 1 that yield steady-state walking at a specified speed \dot{x}_{avg} on a given slope θ . Equality constraints enforce periodicity in the optimization problem. In terms of position of the point mass, $y_i = y_f$ and $d = x_f - x_i$ constrain the forward progression of the point mass to be equal to the distance between touchdown locations of the legs. In terms of point mass velocity, $\dot{y} = 0$ defines the start and end of the step cycle, so the only constraints are that $\dot{x}_i = \dot{x}_f$ and the average velocity over the step matches the specified \dot{x}_{avg} . Equality constraints also enforce continuity of the free lengths of the legs at the gait events where the rates of change of those free lengths are altered. Referring to Fig. 3,

$$\ell_{LO} = \ell_{MS} + \beta_A t_{LO}, \tag{14}$$

$$\ell_{MS} = \ell_{TD} + \beta_B (t_{END} - t_{TD}), \tag{15}$$

TABLE 1: Parameters to be found via solution of the optimization problem.

Description	Parameter
Initial y position	y_i
Initial x velocity	\dot{x}_i
Free length at mid-stance	ℓ_{MS}
Free length at touchdown	ℓ_{TD}
Actual leg length at touchdown	L_{TD}
Free length at lift-off	ℓ_{LO}
Actual leg length at lift-off	L_{LO}
Rates of change in free leg lengths	$\beta_A \& \beta_B$
Leg angle at touchdown	α

where t_{LO} is the time of lift-off of Leg A and t_{END} is the time of mid-stance of Leg B at which the analyzed step ends. Inequality constraints enforce feasibility considerations, such as the actual leg lengths at mid-stance, touchdown, and lift-off being less than or equal to the free lengths at the same points in the gait cycle. No constraints were imposed on the ground reaction forces, but solution gaits in which component of the ground reaction force perpendicular to the ground became negative at any point were discarded as invalid.

The optimization problem was formulated and solved in MATLAB using the *fmincon* command, with *ode45* employed to integrate the equations of motion. The equality and inequality constraints described above were imposed, and the cost function *f* to minimize was

$$f = (\ell_{TD} - L_{TD}) + (\ell_{LO} - L_{LO}). \tag{16}$$

This approach simply minimizes the differences between the actual leg lengths and the free leg lengths at touchdown and lift-off. (The feasibility constraints ensure that each parenthetical quantity is positive, eliminating the need to either square or take the absolute value of each.) In the passive dual-SLIP model, these differences are necessarily equal, so this approach offers consistency across ground slopes. When walking downhill, the actuation acts to absorb energy, and in walking uphill, it injects energy into the system to match the increase in gravitational potential energy. In either case, though, a viable solution with the actuated model could inject or absorb more energy than required by the ground slope with one leg and compensate for that by absorbing or injecting the difference in energy needed with the other leg.

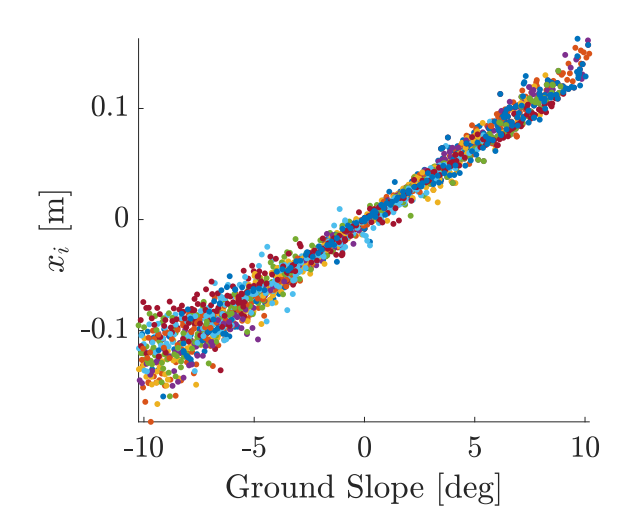
The objective function in Eq. 16 penalizes such solutions to facilitate convergence to an energetically efficient gait in which the two actuated legs do not act in opposition to each other.

For a given speed, a passive seed gait was first computed using the traditional planar dual-SLIP model. From a slope of zero degrees, the ground angle θ was incremented by 0.25 degrees, and a new sloped gait solution was sought. When a feasible solution was found, the ground angle was incremented again, and the most recent solution served as the seed gait for the next ground angle. When no feasible solution was found, the ground angle increment was halved up until a lower bound on $\Delta\theta$ was reached. In such cases, infeasibility established the limit on the ground angle that could be achieved at that speed. Solutions were sought across the range of speeds from $\dot{x}_{avg} = 1.0$ to $1.6 \frac{m}{s}$ in $0.05 \frac{m}{s}$ increments because while self-selected walking speed varies with age and gender, it is typically around 1.3 $\frac{m}{s}$. Solutions were likewise sought across the range of slopes from $\theta = -10$ to 10 degrees to cover slopes up to twice the ADA ramp specification of 4.8 degrees.

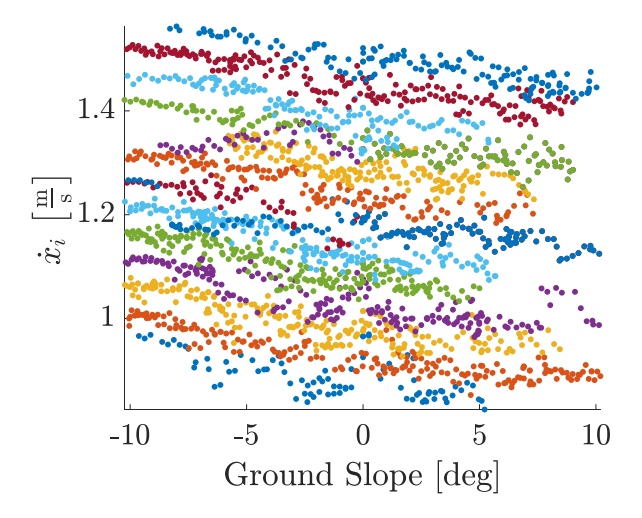
RESULTS

Feasible solution gaits across all speeds and ground slopes were analyzed to identify trends in the gait parameters. Only four of the parameters in Table 1 were consistent enough in the solution gaits to warrant linear regression analysis: x_i , \dot{x}_i , β_A , and β_B . Figure 4 plots the position and velocity of the mass center at the start of the gait cycle, which is mid-stance of the trailing Leg A. As indicated previously, the x position is necessarily zero for flat terrain walking, and not surprisingly, the position increases with increasing walking slope and decreases with decreasing walking slope. As such, mid-stance occurs with the point mass nearly directly above the stance foot in the vertical direction, regardless of ground slope. This is consistent with data showing that humans standing on incline planes reorient their bodies to align the trunk and pelvis with Earth-fixed vertical [9]. Figure 4(a) shows that the variability in x position increases with the magnitude of the ground slope and is higher for declines than inclines. The linear regression data in Table 2 of the Appendix show that the slope and intercept are still quite similar across the entire range of speed.

In fact, the regularity of x_i values in the solution gaits led the authors to explore eliminating it as an optimization variable by enforcing the regression equations in Table 2 at each speed instead. The motivation was to reduce the complexity of the optimization problem and thereby, the computation time, without compromising on solution quality. Regrettably, this approach resulted in far fewer feasible gait solutions, so computation time was actually longer. Seemingly, allowing for small variability in x_i provided the flexibility needed for the optimization to converge to feasible gaits more reliably. As a result, x_i was retained as an optimization parameter.



(a) x position of the center of mass at mid-stance as a function of ground slope and walking speed



(b) x velocity of the center of mass at mid-stance as a function of ground slope and walking speed

FIGURE 4: Position and velocity in the *x*-direction at mid-stance versus ground slope, with each color indicating a different desired walking speed. Subfigure (b) serves as the legend with the slowest speed of $1.0 \frac{m}{s}$ plotted in blue at the bottom and speeds increasing upward to the fastest speed of $1.6 \frac{m}{s}$ plotted in the slightly darker blue at the top.

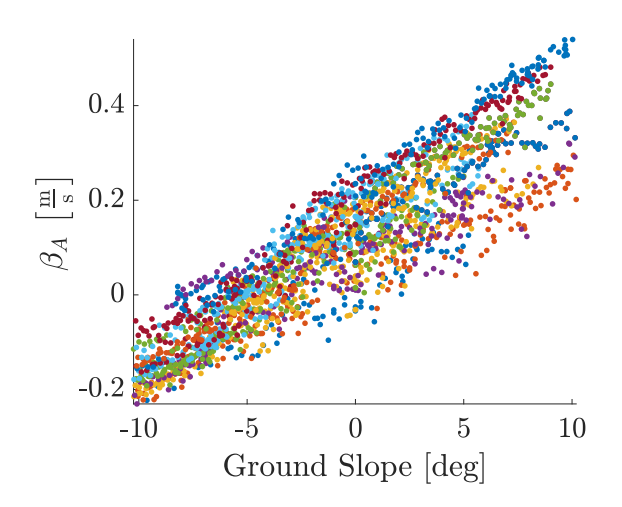
Some variability in initial velocity in the *x*-direction is also seen in Fig. 4(b) across all speeds. Note that in all cases, one would expect the velocity at mid-stance to be smaller than the desired average walking speed since the minimum forward velocity would occur near mid-stance. The linear regression data

in Table 3 of the Appendix show that the slopes of the regression equations are quite similar regardless of the ground slope, but the intercepts of the equations increase monotonically with ground slope, as one would expect. The higher variability in the velocity data is reflected in the lower R^2 values reported in Table 3. Because of the higher variability and the lack of success in reducing the number of optimization parameters by eliminating x_i , no similar effort was made to eliminate \dot{x}_i .

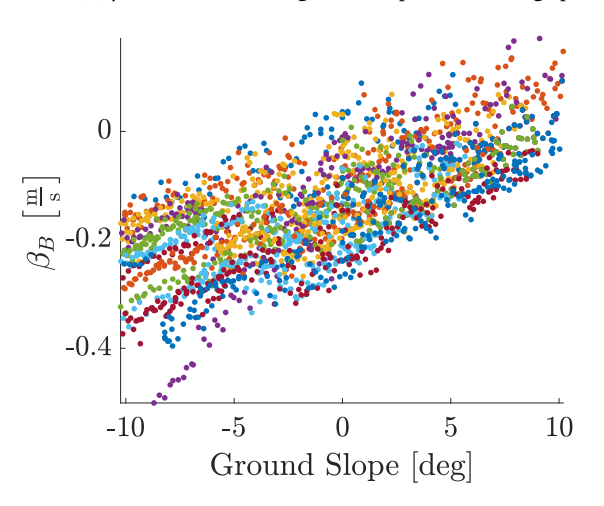
Tables 4 and 5 in the Appendix show that the linear regression model better matched the β_A data than the β_B data plotted in Fig. 5. Both exhibit positive slopes with ground slope, but the β_A slopes generally increase with walking speed, whereas the β_B slopes do not exhibit a consistent trend. In terms of intercept, however, both β_A and β_B have intercepts that increase in magnitude with walking speed, β_B 's being negative. It is not clear why the β_B values exhibit more variability than the β_A values. One hypothesis is that it results from β_A influencing the model's behavior at the start of the gait cycle analysis (mid-stance. Exploring the source of the disparity is a topic of future research.

While other gait parameters were less consistent across speed and ground slope, some trends matching human walking characteristics were observed. First, the duration of stance generally increased with increasing slope across all speeds and decreased with increasing speeds across all slopes. These same trends have been identified in human walking [9, 11], although the model stance duration was generally shorter than the experimental results. Similarly, humans typically descend slopes with a higher step frequency, but modulate step frequency relatively little when ascending inclines [12]. The former at least is consistent with the model behavior. Second, the dual-SLIP model step length increased with increasing slope across all speeds and with increasing speed across all slopes, in agreement with human data [9, 11–14].

Other model trends were inconsistent with human experimental data. For example, the percentage of the gait cycle that the model spent in double support decreased as slope increased across all speeds, and exhibited no consistent trends with speed across all slopes. Opposite effects of slope on double support duration have been observed in humans [13], although the model's 20% of gait cycle spent in double support for a range of slopes at 1.4 $\frac{m}{s}$ did match the human experimental data. Also, the displacement of the model's center of mass in the direction perpendicular to the ground decreased with increasing speed across all slopes, whereas humans typically exhibit an increase in such displacement [15]. Similarly, humans typically shift the peak in ground reaction forces perpendicular to the ground earlier in stance when walking on declines and later in stance when walking on inclines [7, 11, 12, 14]. On declines, the model matched this behavior at the majority of speeds, but exhibited the opposite behavior at some speeds. On inclines, the two peaks of this component of the ground reaction force were roughly equal re-



(a) β_A as a function of ground slope and walking speed



(b) β_B as a function of ground slope and walking speed

FIGURE 5: β_A and β_B versus ground slope, with each color indicating a different desired walking speed as in Fig. 4.

gardless of speed, so the anticipated shift was not observed.

CONCLUSIONS & FUTURE WORK

This paper showed that the actuated planar dual spring-loaded inverted pendulum (dual-SLIP) model can be used to represent walking on flat incline and decline surfaces. By allowing touchdown and lift-off of the legs at lengths different from the free lengths of the leg springs and linear changes in free length from touchdown to mid-stance and mid-stance to lift-off, the model absorbs/injects the energy required to achieve periodic gaits on declines/inclines. Some of the model characteristics match those observed in human slope walking. Stance dura-

tion increased with increasing slope and decreased with increasing speed. Step frequency also increased with decreasing slope, and step length increased with increasing slope and speed. Other model characteristics, however, were inconsistent with human behavior, such as the effect of slope on the percentage of the gait cycle spent in double support and the displacement of the center of mass perpendicular to the ground.

For the actuated dual-SLIP model to serve as a template model for either biped robot control or intent detection in an exoskeleton system, these discrepancies with human behavior should be resolved. The authors hypothesize that most of the discrepancies could be eliminated by working with the 3D dual-SLIP model rather than the planar version explored in this paper because the 3D model allows for lateral sway of the mass center, which is significant, particularly in decline walking. This is a more complex model, however, so one might anticipate increased variability in the nonlinear optimization solutions. Since variability was already an issue identified in this paper, future work will again pursue the model simplification strategies employed unsuccessfully herein to see if superior results can be achieved with the 3D model. An alternative approach to resolving the discrepancies would be to implement a different actuation strategy. For example, rather than modulate the free length, the leg spring stiffness could be altered during the stance phase to absorb or inject energy. Additional actuation variables could also be introduced by assuming a nonlinear change in free length or more frequent modifications of the free length changes with each new phase of gait (i.e. new modifications upon each lift-off and touchdown event, in addition to mid-stance). In all cases, there is a need to trade off model complexity with fidelity of representation of human behavior since the underlying motivation of using the dual-SLIP is its inherent simplicity.

ACKNOWLEDGMENT

This work was supported in part by the National Science Foundation under Grant IIS-1527393.

REFERENCES

- [1] Geyer, H., Seyfarth, A., and Blickhan, R., 2006. "Compliant leg behaviour explains basic dynamics of walking and running". *Proceedings of the Royal Society B: Biological Sciences*, 273(1603), pp. 2861–2867.
- [2] Liu, Y., Wensing, P. M., Orin, D. E., and Zheng, Y. F., 2015. "Dynamic walking in a humanoid robot based on a 3d actuated dual-slip model". In Robotics and Automation (ICRA), 2015 IEEE International Conference on, pp. 5710–5717.
- [3] Liu, Y., Wensing, P. M., Orin, D. E., and Zheng, Y. F., 2015. "Trajectory generation for dynamic walking in a humanoid over uneven terrain using a 3d-actuated dual-slip model".

- In 2015 IEEE/RSJ International Conference on Intelligent Robots and Systems (IROS), IEEE, pp. 374–380.
- [4] Liu, Y., Wensing, P. M., Schmiedeler, J. P., and Orin, D. E., 2016. "Terrain-blind humanoid walking based on a 3-D actuated dual-slip model". *IEEE Robotics and Automation Letters*, 1(2), July, pp. 1073–1080.
- [5] Schmiedeler, J. P., and Wensing, P. M., 2018. "Discussion of a review of intent detection, arbitration, and communication aspects of shared control for physical human-robot interaction(losey, dp, mcdonald, cg, battaglia, e., and o'malley, mk, 2018, asme appl. mech. rev., 70 (1), p. 010804)". *Applied Mechanics Reviews*, 70(1), p. 015503.
- [6] Carda, S., Invernizzi, M., Baricich, A., Cognolato, G., and Cisari, C., 2013. "Does altering inclination alter effectiveness of treadmill training for gait impairment after stroke? a randomized controlled trial". *Clinical Rehabilitation*, 27(10), pp. 932–938.
- [7] Kuster, M., Sakurai, S., and Wood, G., 1995. "Kinematic and kinetic comparison of downhill and level walking". *Clinical Biomechanics*, *10*(2), pp. 79–84.
- [8] Worthen-Chaudhari, L., Bing, J., Schmiedeler, J. P., and Basso, D. M., 2014. "A new look at an old problem: Defining weight acceptance in human walking". *Gait & Posture*, *39*(1), pp. 588–592.
- [9] Leroux, A., Fung, J., and Barbeau, H., 2002. "Postural adaptation to walking on inclined surfaces: I. normal strategies". *Gait & Posture*, *15*(1), pp. 64–74.
- [10] Leroux, A., Fung, J., and Barbeau, H., 2006. "Postural adaptation to walking on inclined surfaces: Ii. strategies following spinal cord injury". *Clinical Neurophysiology*, 117(6), pp. 1273–1282.
- [11] Lay, A. N., Hass, C. J., and Gregor, R. J., 2006. "The effects of sloped surfaces on locomotion: a kinematic and kinetic analysis". *Journal of Biomechanics*, *39*(9), pp. 1621–1628.
- [12] McIntosh, A. S., Beatty, K. T., Dwan, L. N., and Vickers, D. R., 2006. "Gait dynamics on an inclined walkway". *Journal of Biomechanics*, *39*(13), pp. 2491–2502.
- [13] Phan, P. L., Blennerhassett, J. M., Lythgo, N., Dite, W., and Morris, M. E., 2013. "Over-ground walking on level and sloped surfaces in people with stroke compared to healthy matched adults". *Disability and Rehabilitation*, 35(15), pp. 1302–1307.
- [14] Redfern, M. S., and Dipasquale, J., 1997. "Biomechanics of descending ramps". *Gait & Posture*, **6**(2), pp. 119–125.
- [15] Orendurff, M. S., Segal, A. D., Klute, G. K., Berge, J. S., Rohr, E. S., and Kadel, N. J., 2004. "The effect of walking speed on center of mass displacement.". *Journal of Rehabilitation Research & Development*, **41**(6).

Appendix A: Regression Data

TABLE 2: x_i Regression data across all ground slopes.

Speed $\left(\frac{m}{s}\right)$	Slope $\left(\frac{deg}{m}\right)$	Intercept (m)	R^2
1	0.0152	-7.66E-04	0.987
1.05	0.0150	-3.08E-03	0.991
1.1	0.0143	-1.81E-03	0.986
1.15	0.0142	-6.39E-04	0.990
1.2	0.0135	-1.85E-03	0.973
1.25	0.0129	-1.11E-03	0.964
1.3	0.0135	9.95E-04	0.982
1.35	0.0126	-1.96E-04	0.986
1.4	0.0127	-8.42E-04	0.983
1.45	0.0122	3.72E-03	0.983
1.5	0.0118	-2.79E-03	0.964
1.55	0.0114	3.57E-03	0.978
1.6	0.0127	2.84E-03	0.981

TABLE 3: \dot{x}_i Regression data across all ground slopes.

Speed $\left(\frac{m}{s}\right)$	Slope $\left(\frac{deg \cdot s}{m}\right)$	Intercept (m)	R^2
1	-6.06E-03	0.880	0.390
1.05	-5.91E-03	0.930	0.797
1.1	-7.04E-03	0.980	0.698
1.15	-6.74E-03	1.03	0.653
1.2	-8.52E-03	1.08	0.792
1.25	-9.06E-03	1.13	0.810
1.3	-6.78E-03	1.19	0.801
1.35	-7.64E-03	1.24	0.830
1.4	-7.04E-03	1.29	0.626
1.45	-6.80E-03	1.35	0.849
1.5	-9.10E-03	1.38	0.732
1.55	-6.89E-03	1.45	0.830
1.6	-6.43E-03	1.50	0.800

TABLE 4: β_A Regression data across all ground slopes.

Speed $\left(\frac{m}{s}\right)$	Slope $\left(\frac{deg \cdot s}{m}\right)$	Intercept (m)	R^2
1	0.0213	0.0136	0.828
1.05	0.0223	0.0327	0.941
1.1	0.0250	0.0600	0.910
1.15	0.0233	0.0643	0.898
1.2	0.0293	0.105	0.920
1.25	0.0300	0.125	0.947
1.3	0.0285	0.121	0.973
1.35	0.0303	0.146	0.968
1.4	0.0309	0.161	0.939
1.45	0.0299	0.169	0.981
1.5	0.0338	0.204	0.964
1.55	0.0317	0.206	0.978
1.6	0.0325	0.217	0.980

TABLE 5: β_B Regression data across all ground slopes.

Speed $\left(\frac{m}{s}\right)$	Slope $\left(\frac{deg \cdot s}{m}\right)$	Intercept (m)	R^2
1	0.0132	-0.0145	0.654
1.05	0.0126	-0.0402	0.819
1.1	0.0120	-0.0644	0.714
1.15	0.0147	-0.0717	0.778
1.2	0.0103	-0.109	0.623
1.25	0.0104	-0.129	0.715
1.3	0.0137	-0.124	0.888
1.35	0.0127	-0.149	0.836
1.4	0.0127	-0.165	0.709
1.45	0.0150	-0.168	0.919
1.5	0.0120	-0.214	0.717
1.55	0.0150	-0.205	0.879
1.6	0.0171	-0.213	0.915